Bangmod International Journal of Mathematical and Computational Science
https://bangmodmcs.wordpress.com
ISSN : 2408-154X
Bangmod Int. J. Math. & Comp. Sci. Vol. 1 & 2, No. 6, 2020, 25 – 37

QUANTUM RENYI ENTROPY WITH APPLICATION IN IMAGE PROCESSING

Wachirapong Jirakitpuwapat[1,4], **Poom Kumam**[1,2,4,*], **Tanapat Deesuwan**[2,3], **Sompong Dhompongsa**[1,4], **Printaporn Sanguansuttigul**[4]

[1] *KMUTTFixed Point Research Laboratory, Science Laboratory Building, Department of Mathematics, Faculty of Science, King Mongkut's University of Technology Thonburi (KMUTT), 126 Pracha-Uthit Road, Bang Mod, Thrung Khru, Bangkok 10140, Thailand.*
E-mails: wachirapong.jira@hotmail.com, sompong.dho@kmutt.ac.th

[2] *Center of Excellence in Theoretical and Computational Science (TaCS-CoE), Science Laboratory Building, King Mongkut's University of Technology Thonburi (KMUTT), 126 Pracha-Uthit Road, Bang Mod, Thrung Khru, Bangkok 10140, Thailand.*
E-mails: poom.kumam@mail.kmutt.ac.th

[3] *Department of Physics, Faculty of Science, King Mongkut's University of Technology Thonburi (KMUTT), 126 Pracha-Uthit Road, Bang Mod, Thrung Khru, Bangkok 10140, Thailand.*
E-mails: tanapat.dee@kmutt.ac.th

[4] *Department of Mathematics, Faculty of Science, King Mongkut's University of Technology Thonburi (KMUTT), 126 Pracha-Uthit Road, Bang Mod, Thrung Khru, Bangkok 10140, Thailand.*
E-mails: pingprinta0727@gmail.com

**Corresponding author.*

Abstract Thresholding is a basic method for image segmentation. First, we plot a histogram of image to a quantum state. The quantum state represents pixel intensities, and the density matrix represents their probability distribution. Secondly, we plot a histogram of the segment image to a quantum state. The quantum state represents pixel intensities of classes. Finally, we obtain the optimal thresholding by quantum Renyi entropy which explains physical interpretation in quantum language.

MSC: 46N50, 81R50, 80M50
Keywords: histogram, image segmentation, quantum Renyi entropy, quantum state, thresholding.

Submission date: 30.11.2019 / Acceptance date: 13.12.2020 / Available online 31.12.2020

1. Introduction

Biomedical imaging is a technique and process of producing visual representations of areas inside the human body to diagnose medical problems and treatment planning. It has a huge impact on public health. Medical image segmentation is one of the most important parts that helps the doctor to obviously see the region of interest (ROI) of the normal,

diseased anatomy and express the target. It has an important effect on image analysis [1–5]. Digital imaging systems for medical diagnosis are important in health care. Initial digital methods are Magnetic Resonance Imaging (MRI) or Computed Tomography (CT). Radiography is nowadays equipped with digital sensors. Image processing is the popular techniques used for dividing the digital image into multiple parts. The medical image segmentation has played a vital role in scientific research, with the fundamental step to analyze images and extract the data from imaging. In this paper, we focus on Positron Emission Tomography (PET), which is an imaging technique that allow the doctor to see how the organs and tissues are working. The image will collect areas of intensive chemical activity, which is helpful because certain diseases have a higher level of chemical activity. Areas of the disease will show up as bright spots on the PET scan.

In this case, we study Parkinson's disease to make sure how much the concentration of radioactivity is stored in the brain tissue. Parkinson's disease (PD) affects the nerve cells in the midbrain, which is called substantia nigra (putamen and caudate) that produces dopamine which symptoms include muscle rigidity, tremors, and changes in speech and gait. There are several studies on subtle morphological alterations such as atrophy in the putamen and caudate [6–8] After diagnosis, treatments can help relieve symptoms. The objective of segmentation is we want to know the concentration of radioactivity, which is an uptake in brain tissue. Therefore, it is necessary to adopt image segmentation methods to help us to extract the real data from PET imaging. There are so many different ways to perform medical image segmentation, for example, image segmentation applications include imaging data analysis [9–21].

Thresholding is a simple method of image segmentation. There are many advantages such as fast processing and smaller storage space. Quantum mechanisms have been introduced the image processing. There are several applications of quantum image processing such as quantum edge detection [22] and quantum image segmentation [23].

In this paper, we solve the thresholding problem by using quantum state space. The details of the image are represented by the quantum state. We choose the optimal threshold based on the quantum Renyi entropy. The paper is explained as follows: Section 2 gives a description of the image thresholding, Section 3 introduces the criteria of threshold such as between-class variance [24], Shannon entropy [25] and global quantum Renyi entropy, Section 4 provides the experimental results and the last Section is the conclusion.

2. Thresholding

Thresholding [26] is a process in which a group of thresholds are chosen under some criteria, and elements are divided into classes according to the following rule:

$$\ell \to C_i \text{ if } th_{i-1} \le \ell < th_i$$

where $\ell \in [a, b]$ represents the level of elements, $\{th_i : i = 1, \dots, M-1\}$ is the set of thresholds and $\{C_i : i = 1, \dots, M\}$ is the set of classes. Note that $th_0 = a$ and $th_M = b + 1$.

Proposition 2.1. *Suppose that the level of elements is an integer. Assume that* $\{C_i : i = 1, \dots, M\}$ *the set of classes is defined by* $\{th_i : i = 1, \dots, M-1\}$ *the set of thresholds. Then also* $\{C_i : i = 1, \dots, M\}$ *the set of classes is defined by* $\{\lceil th_i \rceil : i = 1, \dots, M-1\}$ *the set of thresholds.*

Proof. Since the level of elements is an integer, $\{C_i : i = 1, \dots, M\}$ the set of classes is defined by $\{th_i : i = 1, \dots, M-1\}$ or $\{\lceil th_i \rceil : i = 1, \dots, M-1\}$ set of thresholds. ∎

3. Criteria of Threshold

In this section, we assume that we divide finite elements into classes by thresholding. Note that TH is a collection of the set of the threshold, i is index classes, ℓ is level of elements, p_ℓ is the probability distribution of element at ℓ-level, ω_i is the probability of occurrence of a class, and μ_i is the mean of a class. So we have

$$\omega_i = \sum_{th_{i-1}\leq \ell < th_i} p_\ell \text{ and } \mu_i = \sum_{th_{i-1}\leq \ell < th_i} \frac{p_\ell}{\omega_i}\ell,$$

where p_ℓ is the probability distribution of element. Remark, if $\omega_i = 0$, then we define $\mu_i = 0$ and $\frac{p_\ell}{\omega_i} = 0$.

3.1. Between-Class Variance

In 1979, Otsu presented the discriminant criterion based on between-class variance [24]. Otsu's algorithm chooses the optimal thresholds by maximizing the function:

$$\arg\max_{(th_1,\ldots,th_{M-1})\in TH} \sum_{i,j=1}^{M} \omega_i\omega_j(\mu_i - \mu_j)^2. \tag{3.1}$$

3.2. Shannon Entropy

In 1985, Kapur presented the discriminant criterion based on Shannon entropy [25]. Kapur's algorithm chooses the optimal thresholds by maximizing the function:

$$\arg\max_{(th_1,\ldots,th_{M-1})\in TH} \sum_{i=1}^{M} H(C_i), \tag{3.2}$$

Note that $H(C_i)$ is the Shannon entropy, which is defined as:

$$H(C_i) = -\sum_{th_{i-1}\leq \ell < th_i} \frac{p_\ell}{\omega_i} log_2 \frac{p_\ell}{\omega_i}.$$

Remark, if $\omega_i = 0$, then we define $H(C_i) = 0$.

3.3. Global Quantum Renyi Entropy (GQRE)

We present the discriminant criterion based on global quantum Renyi entropy. It look like global quantum Von Neumann entropy maximization [27] where $a = 0$.

We represent the histogram of elements with the following:

$$|I> = \sum_{a\leq \ell \leq b} \sqrt{p_\ell}|\theta_\ell > \otimes |\ell >,$$

where we encode the ℓ-th level to $|\theta_\ell >= \cos(\theta_\ell)|0 > + \sin(\theta_\ell)|1 >$, which belongs to the first subsystem (labelled as "A"), by creating a bijective relationship between them, namely

$$\theta_\ell = \frac{\pi}{2}\frac{\ell}{b-a},\ \ell \in [a, b],$$

and $|\ell >$ is the second subsystem (labelled as "B"), which denotes the indices of the element. The density matrix for the first subsystem A defined by:

$$\rho = \sum_{a\leq \ell \leq b} p_\ell |\theta_\ell >< \theta_\ell|.$$

It contains information about the probability distribution of elements.

We represent the histogram of the segmented element with the following:

$$|I' >= \sum_{i=1}^{M} \left(\sqrt{\omega_i}|\theta_i' > \otimes \sum_{th_{i-1} \leq \ell < th_i} \sqrt{\frac{p_\ell}{\omega_i}}|i > \right),$$

where we encode the i-th class to $|\theta_i' >= \cos(\theta_i')|0 > +\sin(\theta_i')|1 >$, which belongs to the first subsystem (labelled as "A'"), by creating a bijective relationship between them, namely

$$\theta_i' = \frac{\pi}{2} \frac{\mu_i}{b-a}.$$

$|i >$ is the second subsystem (labelled as "B'"), which denotes the indices of the element in the class. Remark, if $\omega_i = 0$, then we define $\sqrt{\frac{p_\ell}{\omega_i}} = 0$. The density matrix for the first subsystem A' defined by:

$$\rho' = \sum_{i=1}^{M} \omega_i |\theta_i' >< \theta_i'|.$$

It contains information about the probability of the occurrence of classes. So the quantum Renyi entropy of ρ' [28, 29]:

$$S_\alpha(\rho') = \frac{1}{1-\alpha} In(Tr(\rho'^{\alpha})) = \frac{1}{1-\alpha} ln(\lambda_1^\alpha + \lambda_2^\alpha),$$

where λ_1 and λ_2 are eigenvalues of ρ' such that $\alpha \in [0,1) \cup (1,\infty)$. The optimal thresholds are maximizing function:

$$\arg\max_{(th_1,\ldots,th_{M-1}) \in TH} S_\alpha(\rho'). \tag{3.3}$$

It is called the "Global Quantum Renyi Entropy".

Remark 3.1. [29] Let $\{\alpha_n\}$ be a sequence that converges to 1. Then $\{S_{\alpha_n}(\rho)\}$ is a sequence of quantum Renyi entropy converse to $S(\rho)$ quantum Von Neumann entropy :

$$S(\rho) = -Tr(\rho ln \rho) = -\lambda_1 ln(\lambda_1) - \lambda_2 ln(\lambda_2),$$

where λ_1 and λ_2 are eigenvalues of ρ.

4. Experiment

4.1. Test Images

The cameraman picture with size 256×256 was tested, see Figures 1 and 2. This picture is small in size and has less number of pixel level. We divide it into 2 classes, and compute the value of the criteria. See Figures 3, 5, 7, 9, 11, 13 and 15. Then we get results. See Figures 4, 6, 8, 10, 12, 14 and 16. Table 1 shows the time of computing algorithms.

Figure 1. Original

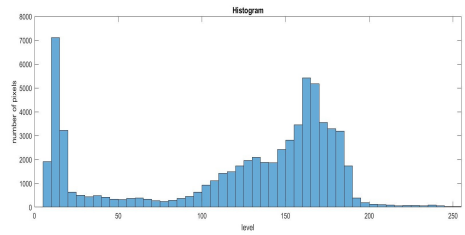

Figure 2. Histogram

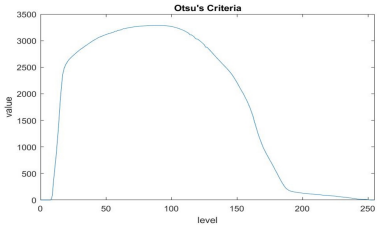

FIGURE 3. Otsu's Criteria

FIGURE 4. Otsu's Result

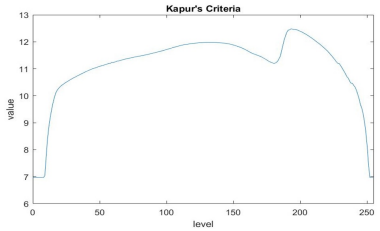

FIGURE 5. Kapur's Criteria

FIGURE 6. Kapur's Result

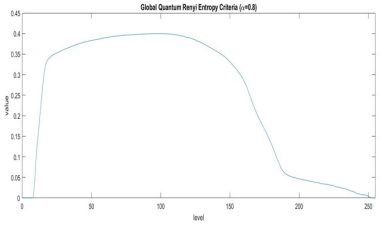

FIGURE 7. Global Quantum Renyi Entropy Criteria ($\alpha = 0.8$)

FIGURE 8. Global Quantum Renyi Entropy Result ($\alpha = 0.8$)

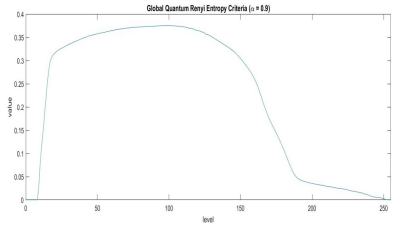

FIGURE 9. Global Quantum Renyi Entropy Criteria ($\alpha = 0.9$)

FIGURE 10. Global Quantum Renyi Entropy Result ($\alpha = 0.9$)

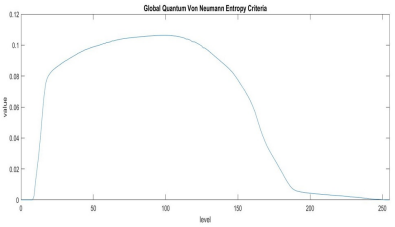

FIGURE 11. Global Quantum Von Neumann Entropy Criteria

FIGURE 12. Global Quantum Von Neumann Entropy Result

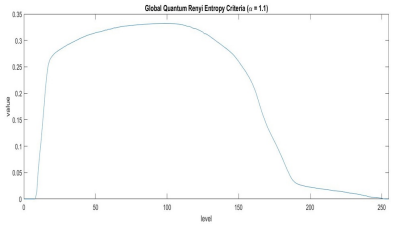

FIGURE 13. Global Quantum Renyi Entropy Criteria ($\alpha = 1.1$)

FIGURE 14. Global Quantum Renyi Entropy Result ($\alpha = 1.1$)

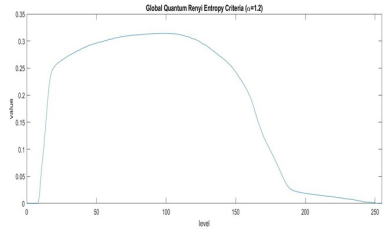

FIGURE 15. Global Quantum Renyi Entropy Criteria ($\alpha = 1.2$)

FIGURE 16. Global Quantum Renyi Entropy Result ($\alpha = 1.2$)

Criteria	Time (sec)
Between-Class Variance	0.039049
Shannon Entropy	0.039827
Global Quantum Renyi Entropy ($\alpha = 0.8$)	0.038152
Global Quantum Renyi Entropy ($\alpha = 0.9$)	0.037357
Global Quantum Von Neumann Entropy	0.039463
Global Quantum Renyi Entropy ($\alpha = 1.1$)	0.038237
Global Quantum Renyi Entropy ($\alpha = 1.2$)	0.039148

TABLE 1. Time

4.2. Brain X-Ray

Brain X-Ray with size 336×336 was tested, see Figure 17. We want a bright area in Figure 17. Figure 18 is a rescaled brain X-ray. Figure 19 and 20 are histograms of Figure 17 and 18, respectively. we want to separate three groups without zero pixels or background. The first group is noisy, the second area of the brain is not bright, and the third area of the brain is bright. Since the original image has a lot of the number of pixel level (intensive chemical) and are separated into three groups, then the process of finding the threshold will be very slow. Therefore, we need to find a threshold from the rescaling image. Although we use thresholding, we necessary delete small areas in the image after thresholding. See Figures 21, 22, 23, 24, 25, 26 and 27. Figures 28 and 29 are reference image for comparing algorithms. Table 2 shows the time of computing algorithms, PSNR and SNR.

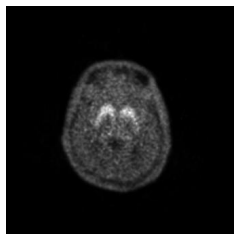

Figure 17. Original Brain

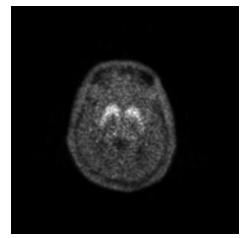

Figure 18. Rescale Brain

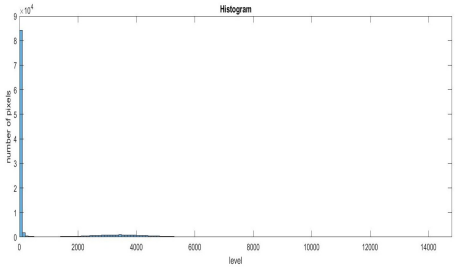

Figure 19. Histogram Original Brain

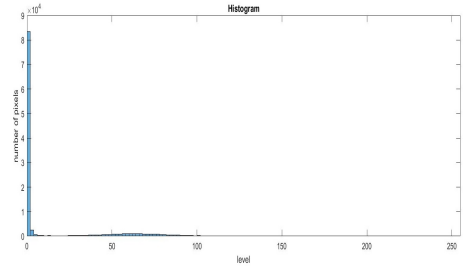

Figure 20. Histogram Rescale Brain

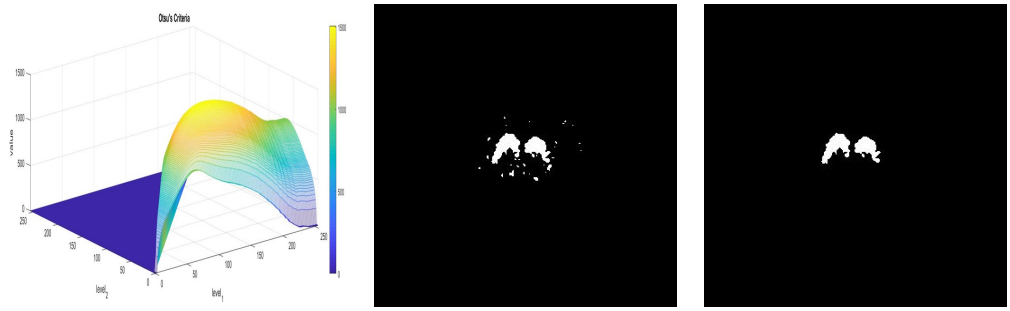

(A) (B) (C)

FIGURE 21. Figure (a), (b) and (c) show the Otsu's criteria, thresholding result and result without noise, respectively.

(A) (B) (C)

FIGURE 22. Figure (a), (b) and (c) show the Kapur's criteria, thresholding result and result without noise, respectively.

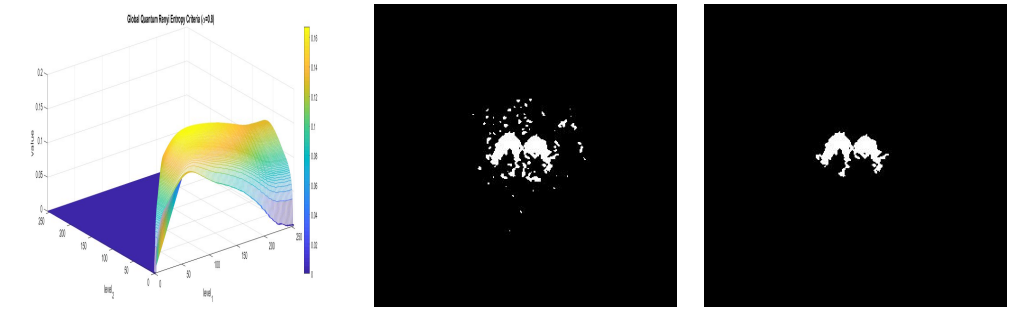

(A) (B) (C)

FIGURE 23. Figure (a), (b) and (c) show the Global Quantum Renyi Entropy criteria ($\alpha = 0.8$), thresholding result and result without noise, respectively.

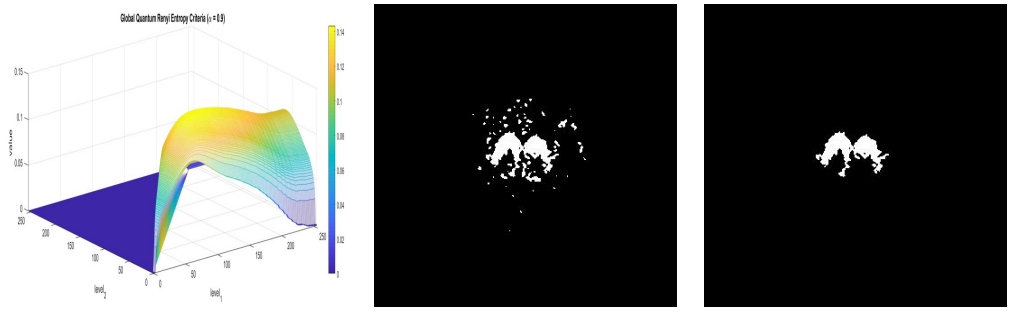

(A) (B) (C)

FIGURE 24. Figure (a), (b) and (c) show the Global Quantum Renyi Entropy criteria ($\alpha = 0.9$), thresholding result and result without noise, respectively.

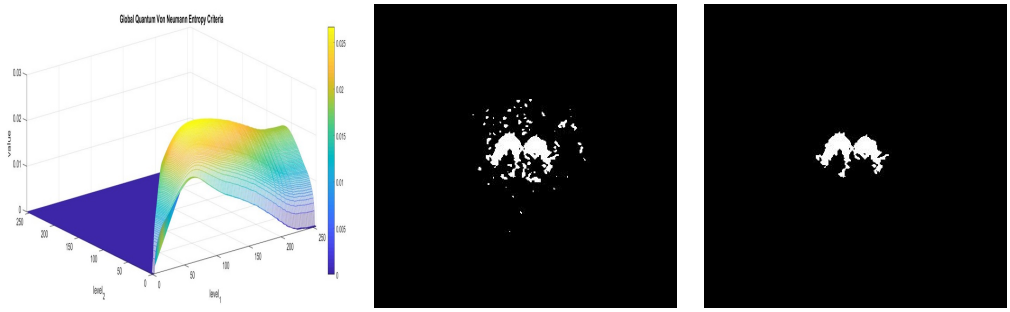

(A) (B) (C)

FIGURE 25. Figure (a), (b) and (c) show the Global Quantum Von Neumann Entropy criteria, thresholding result and result without noise, respectively.

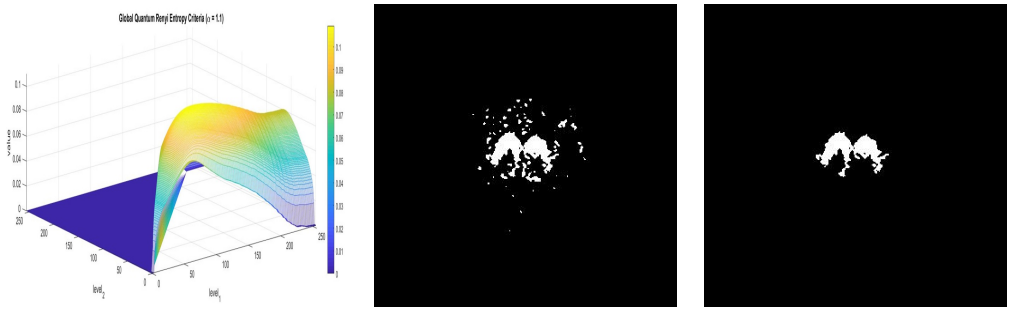

(A) (B) (C)

FIGURE 26. Figure (a), (b) and (c) show the Global Quantum Renyi Entropy criteria ($\alpha = 1.1$), thresholding result and result without noise, respectively.

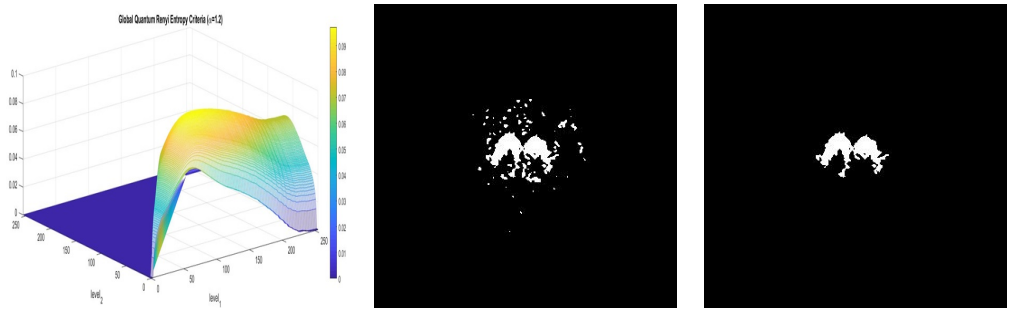

(A) (B) (C)

FIGURE 27. Figure (a), (b) and (c) show the Global Quantum Renyi Entropy criteria ($\alpha = 1.2$), thresholding result and result without noise, respectively.

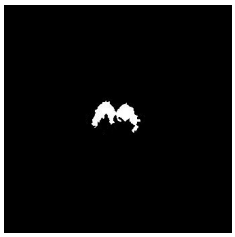

FIGURE 28. Reference Area

FIGURE 29. Reference Brain

Criteria	Time (sec)	PSNR	SNR
Between-Class Variance	4.252742	31.6596	7.9733
Shannon Entropy	4.814529	26.2509	2.5645
Global Quantum Renyi Entropy ($\alpha = 0.8$)	2.028647	36.3647	12.6783
Global Quantum Renyi Entropy ($\alpha = 0.9$)	1.908024	36.3647	12.6783
Global Quantum Von Neumann Entropy	2.313753	36.3647	12.6783
Global Quantum Renyi Entropy ($\alpha = 1.1$)	2.157493	36.3647	12.6783
Global Quantum Renyi Entropy ($\alpha = 1.2$)	2.543781	36.3647	12.6783

TABLE 2. Compare

5. Conclusion

We solve the image thresholding problem by using quantum Renyi entropy. First, we plot histogram of elements to a quantum state. The quantum state represents elements intensities and the density matrix represents their probability distribution. Secondly, we plot histogram of the segment elements to a quantum state which represents elements intensities of classes. The optimal threshold is divided into classes that is the largest quantum information. We presented new criteria called global quantum Renyi entropy maximization. It determines the optimal thresholds in the quantum language. Sometimes, elements have a lot of the number of pixel level and we want to separate them into many groups. Thus the process of finding threshold become very slow. Therefore, we find a threshold from the rescaling elements.

Conflict of Interests

The author declare that there is no conflict of interests regarding the publication of this paper.

References

[1] M. Bhat, *Digital image processing*, Int. J. Sci. Technol. **3** (2014), 272–276.

[2] M. Z. Nida, J. A. Musbah, *Survey on Image Segmentation Techniques*, Procedia Computer Science, **65** (2015), 797–806.

[3] S. Becker, M. Plumbley, *Unsupervised neural network learning procedures for feature extraction and classification*, J Appl Intell. **6** (1996), 185.

[4] R. Beichel, H. Bischof, F. Leberl, M. Sonka, *Robust active appearance models and their application to medical image analysis*, IEEE Trans Med Imaging, **24** (2005), 1151.

[5] T. McInerney, D. Terzopoulos, *A dynamic finite element surface model for segmentation and tracking in multidimensional medical images with application to cardiac 4D image analysis*, Comput Med Imaging Graph, **19** (1995), 69.

[6] M. Ghaemi, R. Hilker, J. Rudolf, J. Sobesky, W. D. Heiss, *Differentiating multiple system atrophy from Parkinson's disease: contribution of striatal and midbrain MRI volumetry and multi-tracer PET imaging*, Journal of Neurology, Neurosurgery & Psychiatry, **73** (2002), 517–523.

[7] A. Garg, S. A. Cresswell, K. Popuri, M. J. McKeown , M. F. Beg, *Morphological alterations in the caudate, putamen, pallidum, and thalamus in Parkinson's disease*, Frontiers in Neuroscience, **9** (2015), 101.

[8] T. L. Pitcher, T. R. Melzer, M. R. MacAskill, et al., *Reduced striatal volumes in Parkinson's disease: a magnetic resonance imaging study*, Translational Neurodegeneration, **1** (2012) 1–17.

[9] M. Kamel, A. Zhao, *Extraction of Binary Character/Graphics Images from Grayscale Document Images*, CVGIP: Graph. Models Image Process, **55** (1993), 203–217.

[10] S. Saha, S. Bandyopadhyay, *Automatic MR brain image segmentation using a multiseed based multiobjective clustering approach*, Applied Intelligence, **35** (2011), 411–427.

[11] E. Cuevas, F. Sención, D. Zaldivar, P. C. Marco, H. Sossa, *A multi-threshold segmentation approach based on Artificial Bee Colony optimization*, Applied Intelligence, **37** (2012), 321–336.

[12] M.N. Ahmed, S. M. Yamany, N. Mohamed, A. A. Farag, T. Moriarty, *A modified fuzzy C-means algorithm for bias field estimation and segmentation of MRI data*, IEEE Trans Med Imaging. **21** (2002), 193.

[13] J. Alirezaie, M.E. Jernigan, C. Nahmias, *Neural network-based segmentation of magnetic resonance images of the brain*, IEEE Trans Nuclear Sci. **44** (1997), 194.

[14] R. V. Andreao, J. Boudy, *Combining wavelet transform and hidden Markov models for ECG segmentation*, EURASIP J Appl Signal Process. (2007), 95.

[15] J.C. Bezdek, L.O. Hall, L.P. Clarke, *Review of MR image segmentation techniques using pattern recognition*, Med Phys. **20** (1993), 1033.

[16] B. Biswal, N. Shah, N. Shah, M. Trivedi, S. Nayak, H. Dave. *Automatic segmentation of pancreatic images using ISODATA algorithm*, J Clin Oncol 2006 ASCO Annu Meet Proc. **24** (2006) 141–149.

[17] WL Cai, SC Chen, DQ Zhang. Fast and robust fuzzy C-means clustering algorithms incorporating local information for image segmentation. *Pattern Recognit.* 2007;40:825.

[18] K. S. Cheng, J. S. Lin, C. W. Mao, *The application of competitive Hopfield neural network to medical image segmentation*, IEEE Trans Med Imaging. **15** (1996), 560.

[19] P. C. Gonalves, J. M. Tavares, R. M. Jorge, *Segmentation and simulation of objects represented in images using physical principles*, Comput Model Eng Sci. **32** (2008), 45.

[20] V. Grau, A. U. Mewes, M. Alcaniz, R. Kikinis, S. K. Warfield, *Improved watershed transform for medical image segmentation using prior information*, IEEE Trans Med Imaging. **23** (2004), 447.

[21] C. L. Guyader, L. A. Vese, *Self-repelling snakes for topology-preserving segmentation models*, IEEE Trans Image Process. **17** (2008), 767.

[22] Y. Sun, *Quantum Statistical Edge Detection Using Path Integral Monte Carlo Simulation*, Bio Inspired Computing Theories and Applications, Springer Berlin Heidelberg, 2014.

[23] S. Caraiman, V. I. Manta, *Image segmentation on a quantum computer*, Quantum Information Processing, **14** (2015), 1693–1715.

[24] N. Otsu, *A Threshold Selection Method from Gray-Level Histograms*, IEEE Transactions on Systems, Man, and Cybernetics, **9** (1979), 62–66.

[25] J. N. Kapur, P. K. Sahoo , A. K. C. Wong, *A new method for gray-level picture thresholding using the entropy of the histogram*, Computer Vision, Graphics, and Image Processing, **29** (1985), 273–285.
[26] D. Sundararajan, *Digital Image Processing: A Signal Processing and Algorithmic Approach*, Springer Publishing Company, Incorporated, 2017.
[27] X. Wang, C. Yang, G. S. Xie, Z. Liu, *Image Thresholding Segmentation on Quantum State Space*, Entropy, **10** (2018), 20.
[28] M. B. Bassat, J. Raviv, *Renyi's entropy and the probability of error*, IEEE Transactions on Information Theory, **24** (1978), 324–331.
[29] X. Hu, Z. Ye, *Generalized quantum entropy*, Journal of Mathematical Physics, **47** (2006), 023502.

References should be cited in the text as, e.g., [5], [6, p. 213], or [6, Theorem 2.1]. It is suggested that the theorem and page numbers be used for referencing instead of just a number representing an entire book or paper, and also that only those papers or books which are actually cited in the text be listed as references.